High-Durability Hydrogen Combustion Engines: A Comparative Study of Cast Irons and Steels

Rafael Brisolla Obara
Anna Louise Voigt
André Ferrarese
Carlos de Souza Cabezas
Tupy S.A.

Luiza de Brito Fantin
Marcelo Ferreira Moreira
Anna Ramus Moreira
Luís Fernando Fiuza Chaves
Instituto de Pesquisas Tecnológicas

ABSTRACT

The global shift toward decarbonization has positioned hydrogen (H_2) as a key energy vector. In combustion engines, especially for commercial vehicles, H_2 offers high efficiency at full load, tolerance to low-purity H_2, lower costs, and improved durability over other zero-emission solutions. A key challenge is selecting materials that withstand hydrogen induced damage – a process that reduces toughness and increases cracking risk. Austenitic stainless steels resist hydrogen damage but are costly and have limited wear resistance. High-strength steels offer greater strength at lower costs but are more prone to hydrogen damage. Cast irons emerge as a promising alternative, combining strength, cost-effectiveness, thermal properties, and low susceptibility to hydrogen damage due to graphite. This study investigates high temperature hydrogen attack (HTHA) mechanism in cast irons and forged steels. Samples were hydrogenated in an autoclave for over 2,000 hours at 300 bar and 375°C, simulating severe H_2 engine conditions. Results confirmed the superior resistance of cast irons. Additionally, findings were compared with global standards for H_2 combustion engines, providing insights into material selection strategies to ensure high durability in future applications.

INTRODUCTION

The increase in greenhouse gas emissions has accelerated global warming, intensifying extreme weather events, raising sea levels, and impacting ecosystems and economies on a global scale [1]. In response, the international community has adopted more ambitious emission reduction commitments, as outlined in the Paris Agreement [2]. This agreement aims to limit the rise in average global temperature, while COP29 reinforced climate financing by establishing that developed nations must allocate USD 300 billion annually until 2035 to support energy transition and climate adaptation efforts [3].

Among the sectors requiring the most significant decarbonization efforts, transportation stands out as one of the largest sources of CO_2 emissions [4]. The combustion of fossil fuels in the transport sector remains a significant contributor to global emissions, making it a central challenge against climate change. Several alternatives have been developed to make mobility more sustainable, including the use of biofuels such as ethanol and biomethane, as well as low-carbon hydrogen [5–8]. The latter, in particular, has emerged as a promising solution – especially for heavy-duty vehicles, where electrification faces technical and economic limitations [9].

Unlike regular fuels, hydrogen combustion does not produce direct CO_2 emissions, making it a promising alternative for the energy transition. In addition to being a more cost-effective solution than fuel cells, hydrogen internal combustion engines share approximately 90% of their components with conventional internal combustion engines. This technical compatibility facilitates the integration of the new system into existing manufacturing chains, reducing adaptation costs and supporting large-scale adoption. Besides costs, combustion engine presents high performance at full load, higher durability (3 to 5x higher) and enables the use of hydrogen with lower purity.

Reflecting this potential, most heavy-duty vehicle manufacturers have already announced hydrogen engine development projects [10–27]. In some regions, the viability of this technology is also being explored for light-duty vehicles, further expanding its role in sustainable mobility [28]. However, the use of H_2 as a fuel introduces challenges in the selection of materials for engine structural components. One of the main obstacles is hydrogen-induced damage, a set of processes that reduce the load-bearing capacity of the material [29–30].

Hydrogen-induced damage can lead to crack formation due to a combination of internal pressure buildup, weakened interatomic bonding, and increased dislocation mobility. As a result, mechanical strength is compromised, potentially leading to premature component failure [29–30]. Susceptibility to hydrogen damage depends on factors such as temperature, pressure, hydrogen concentration or pH, and the material's microstructure [31], making proper material selection a critical aspect in the development of durable and efficient hydrogen combustion engines.

Currently, austenitic stainless steels are widely used in hydrogen-related applications due to their high resistance to hydrogen-induced damage [32]. However, their high cost, low wear resistance, and limited thermal conductivity constrain their viability for components exposed to severe operating conditions [33–36]. High-strength steels, on the other hand, offer lower cost and greater mechanical strength but are more susceptible to hydrogen damage [37–38].

In this context, cast irons emerge as promising alternatives, offering a combination of good mechanical strength, superior thermal properties, and competitive cost [39–40]. Studies indicate that the presence of graphite in cast irons can act as a trap for hydrogen, reducing its diffusion and, consequently, the effects of hydrogen-induced damage [41]. Additionally, high silicon content in cast irons may form further barriers to hydrogen absorption, enhancing the material's resistance [42–44].

Given these factors, the present study provides a comparative analysis of cast irons and steels employed in hydrogen internal combustion engines, focusing on their susceptibility to hydrogen-induced damage, their mechanical properties, and the long-term viability of these materials. As part of a research project funded by Embrapii and developed in partnership with the Institute for Technological Research of the State of São Paulo (IPT), cast iron and steel samples were hydrogenated in an autoclave at 300 bar and 375°C for over 2,000 hours, simulating extreme operating conditions.

HYDROGEN-INDUCED DAMAGE

Hydrogen can cause various types of damage in metallic alloys, involving a range of chemical processes that compromise material integrity [29–30]. Among the most significant effects are the formation of molecular hydrogen and gaseous byproducts resulting from reactions between hydrogen and alloying elements or impurities, the development of hydrogen solid solutions, and the precipitation of brittle intermetallic hydrides [29–30]. These processes can degrade the mechanical properties of materials and contribute to premature failure, making the study of hydrogen behavior in metallic alloys essential for the development of materials with improved resistance to embrittlement.

The primary mechanisms associated with hydrogen damage include hydrogen-induced blistering/cracking, cracking from precipitation of internal hydrogen, cracking from hydride formation, and high temperature hydrogen attack [29]. Each of these mechanisms represents a distinct mode of interaction between hydrogen and metal, impacting strength and durability in different ways.

Hydrogen-induced cracking or blistering typically occurs in low carbon steels at low temperatures and may also manifest when the material is exposed to cathodic reactions [45]. In this form of damage, hydrogen atoms diffuse into the material and accumulate at incoherent interfaces. The damage is characterized by the formation of blisters or even cracks caused by the buildup of diatomic hydrogen (H_2) [29, 45–46]. These blisters can expand and coalesce, generating internal stresses that may lead to surface cracking. Cracks, in turn, can propagate under stress, potentially resulting in catastrophic failure [31]. For this reason, hydrogen-induced cracking is particularly problematic in materials subjected to high stress, such as in high-pressure environments or components under significant mechanical loads [47].

The precipitation of internal hydrogen occurs especially during melting or welding processes, due to hydrogen absorption in the molten metal [29]. As the material solidifies, the solubility of hydrogen decreases, leading to its precipitation at structural defects such as voids and pores. Similar to hydrogen-induced cracking or blistering, the increase in pressure at the precipitation sites generates internal stresses that can promote crack propagation. These hydrogen-related fractures are commonly referred to as fisheyes, flakes, or shatter cracks [29, 31].

The formation of intermetallic hydrides occurs when hydrogen reacts with Zr, Ti, Ta and others transition metals, rare earth elements, or alkaline earth metals to form metal hydrides – hard and brittle compounds that may increase mechanical strength but significantly reduce the ductility and toughness of the alloy [29]. The presence of hydrides can substantially weaken the material's structure, particularly under conditions of high hydrogenation pressure or elevated temperatures, where hydride formation is thermodynamically favored [31].

High temperature hydrogen attack (HTHA) takes place when hydrogen reacts with metallic components at elevated temperatures, leading to a progressive and irreversible loss of strength, ductility, and toughness [29]. In this process, atomic hydrogen is absorbed and accumulates in interfaces and other defects. It subsequently recombines into molecular hydrogen and reacts with carbon present in carbides or in solid solution. This thermodynamically favorable reaction, occurring at temperatures between 200 and 600°C, produces methane. Due to its relatively large molecular size, methane cannot diffuse out of the microstructure and becomes trapped as bubbles [31]. The continued growth of these bubbles leads to the coalescence of microvoids, the formation of microcracks, and ultimately the linking of these cracks into intergranular fractures. Intergranular cracking reduces the load-bearing cross-sectional area and can eventually result in material failure [29, 31]. Figure 1 shows the formation of bubbles along grain boundaries, with sizes ranging from 0.1 to 1.0 µm, as a result of HTHA-induced degradation in ferrous alloys, which is depicted in Figure 2.

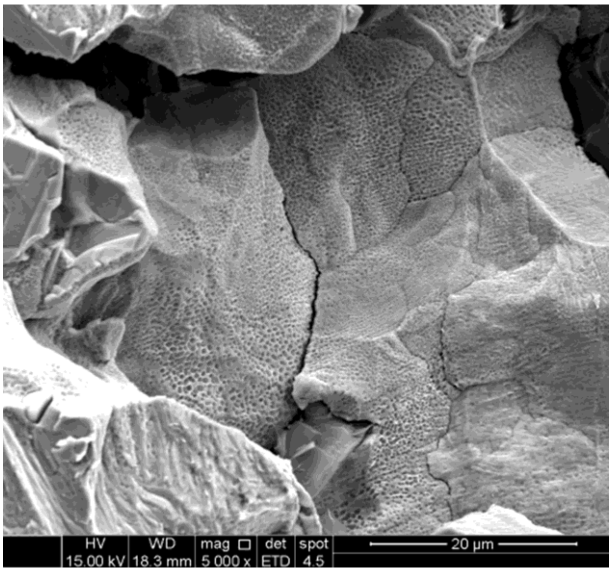

Figure 1. Formation of gas bubbles along grain boundaries in a ferrous alloy as a result of HTHA

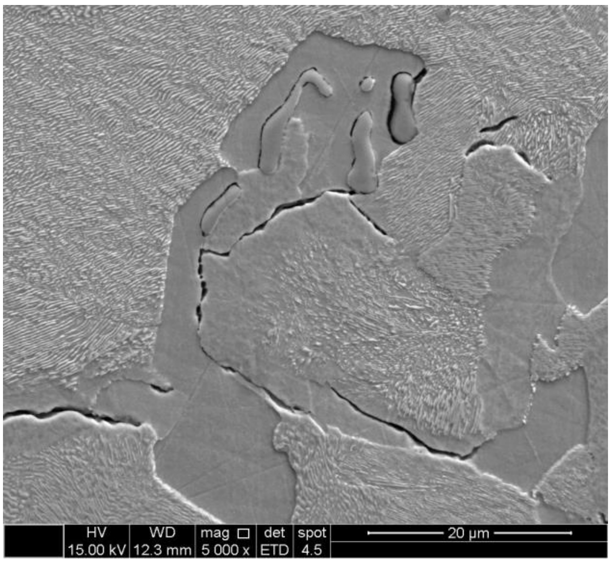

Figure 2. HTHA damage along grain boundaries in a ferrous alloy

HTHA typically occurs at temperatures above 200°C and pressures exceeding 7 bar. The severity of this form of degradation depends on several factors, including temperature, hydrogen partial pressure, exposure time, applied stress, and the alloy's composition and microstructure [31]. In general, the relevance of this embrittlement mechanism lies in its potential to cause failure, particularly in reactors and equipment used in the chemical and petrochemical industries, as well as in hydrogen internal combustion engines [29, 48].

Resistance to HTHA is commonly assessed using Nelson curves, which define safe operational limits in terms of temperature and hydrogen partial pressure for selected alloys. These curves show that alloys containing strong carbide-forming elements, such as chromium and molybdenum, tend to exhibit lower susceptibility to HTHA, as these elements enhance carbide stability. Although Nelson curves are a valuable tool for evaluating HTHA resistance, their applicability is limited to a relatively narrow range of materials [29, 31].

In the experiments described in this study, hydrogenation was conducted under severe temperature and pressure conditions, promoting the onset of HTHA. This failure mode is widely recognized as the predominant mechanism of embrittlement in hydrogen-fueled internal combustion engines and, for this reason, represents the central focus of this investigation [48]. Accordingly, this work emphasizes the analysis of hydrogen interaction mechanisms with alloying elements or impurities within the metallic matrix at elevated temperatures, leading to the formation of gaseous products and the consequent microstructural degradation of the tested materials.

HYDROGEN TRAPPING SITES

In metallic materials, hydrogen trapping occurs predominantly at sites with high binding energy, commonly referred to as traps. These traps can be classified as either reversible or irreversible, depending on the binding energy of hydrogen at the location where it is retained [49]. Major trapping sites include dislocations, grain boundaries, vacancies, non-metallic inclusions, precipitates, and structural defects such as cracks and microvoids [50–51]. The presence and density of these traps significantly influence hydrogen diffusion mechanisms and mobility, thereby affecting the material's susceptibility to embrittlement [50–53].

In cast irons, the presence of graphite not only influences mechanical and thermal properties but also provides a notable advantage over steels by enhancing resistance to hydrogen damage. While hydrogen tends to diffuse more freely through the metallic matrix in steels, in cast irons, graphite particles act as trapping sites for hydrogen [39, 41, 54–55]. These sites serve as high-energy traps where hydrogen is stably retained, reducing its mobility and preventing it from reaching critical regions of the microstructure, such as grain boundaries or areas under high stress [56–57]. Consequently, the morphology, distribution, and size of graphite particles play a significant role in this behavior and are key factors in determining the performance of cast irons in hydrogen-rich environments [58].

Cast irons exhibit a high hydrogen desorption rate at temperatures up to 200°C, with graphite particles being one of the main contributors to this phenomenon [57]. In hydrogen-fueled internal combustion engines, this characteristic provides an additional advantage: during periods when the engine remains hot after shutdown, graphite facilitates the controlled release of previously absorbed hydrogen. Under such conditions, part of the trapped hydrogen can desorb back into the environment, especially when graphite is located near the material surface. This highlights a particularly beneficial property of graphite: in addition to serving as stable trapping sites, graphite particles also act as preferential pathways for desorption, promoting the removal of hydrogen from the microstructure. This “self-relieving” capability helps reduce hydrogen accumulation over time, thereby enhancing the durability of components subjected to thermal cycling typical of intermittent operation.

As a strong graphitizing agent, silicon is also widely used in the composition of major cast iron grades [59]. As a result, these materials typically contain significantly higher silicon contents than steels. Like graphite, silicon reduces hydrogen solubility in the crystalline lattice and restricts its diffusion through the matrix due to the formation of surface oxide layers [42–44].

MATERIALS AND METHODS

Specimens for tensile and impact testing were fabricated from two forged steel alloys (DIN 38Mn6 and DIN 42CrMo4) and a gray cast iron class 250 (FC250). The specimens were subjected to hydrogenation in an autoclave for 2,160 hours, under a pressure of 300 bar and a temperature of 375°C, using hydrogen with 99.9% purity. This procedure aimed to simulate, under controlled laboratory conditions, operational environments representative of hydrogen-powered engines, corresponding to an estimated service life of 1,500,000 km.

To prevent contact between the specimens and the internal walls of the pressure vessel, they were positioned on inert supports made from 99% pure alumina (see Fig. 3). Every 540 hours of exposure, three specimens from each material were removed for mechanical testing.

The mechanical characterization tests were conducted in triplicate. Tensile tests followed the ISO 6892 standard [60], using an Instron 300 DX universal testing machine. Charpy impact tests were conducted at room temperature in accordance with ASTM E23 [61], using a Wolpert testing machine with a 150 J capacity. The specimens measured 55 × 10 × 10 mm, featuring a V-notch for forged steels, while unnotched samples were used for the cast irons.

Figure 3. Alumina supports for positioning the specimens in the autoclave

RESULTS AND ANALYSIS

Figure 4 graphically presents the tensile strength limits of the three materials evaluated over the course of hydrogen exposure. As expected, the forged steels exhibited a significant reduction in this parameter, highlighting the microstructural degradation caused by methane formation in grain boundaries. The largest variation was observed for the 38Mn6 steel, whose tensile strength was reduced to less than half of its original value. It is noticeable that this material experienced a sharp decline in the first few hours of exposure, indicating a low resistance to hydrogen attack, possibly related to a small number of high-energy trapping sites and low stability carbides in the microstructure.

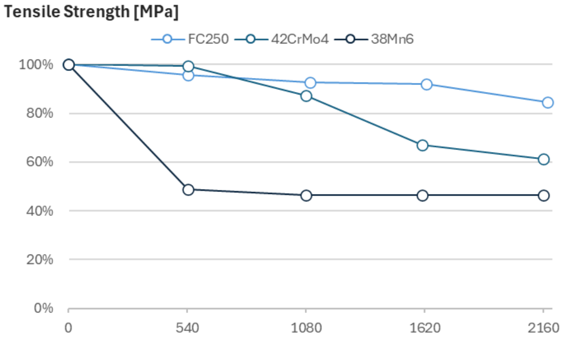

Figure 4. Percentage reduction in tensile strength after up to 2,160 hours of hydrogen exposure

The 42CrMo4 steel, in turn, exhibited the best performance among the steels evaluated, with a 39% reduction in tensile strength after 2,160 hours of hydrogen exposure. Its chemical composition, containing 0.87% Cr and 0.16% Mo, contributes to lower susceptibility to HTHA. These elements form stable carbides, which are more thermodynamically stable than cementite, enhancing resistance to HTHA [62]. For this reason, Cr and Mo are widely used in alloys with high resistance to HTHA [29,31]. Nevertheless, the material experienced considerable mechanical degradation, highlighting that even with strategic alloying element additions, prolonged exposure to hydrogen can significantly compromise the performance of forged steels.

In contrast to the behavior observed in the steels, the FC250 gray cast iron showed much better performance in terms of resistance to hydrogen attack. It is worth noting that this material is widely used in the automotive industry due to its low cost and excellent processability, not having been optimized for applications involving hydrogen-containing environments. Still, the FC250 exhibited only a 15% reduction in tensile strength after the entire exposure period – less than half the variation observed for the 42CrMo4 steel. Furthermore, until 1,620 hours of exposure, the material maintained a tensile strength greater than 250 MPa, staying within the regulatory requirements for the FC250 class. This performance may be primarily attributed to the presence of graphite in its microstructure, which acts as high-energy traps for hydrogen and hinders its diffusion in the metallic matrix, contributing to the thermodynamic stability of the material even under aggressive hydrogen exposure conditions. A minor contribution may also stem from the residual chromium content below 0.3%, which might have played a subtle role in enhancing the material's overall resistance to hydrogen-induced degradation through the formation of more stable carbides.

Figure 5 shows the results of the absorbed energy in Charpy impact tests. Similarly to what was observed in the tensile tests, the 38Mn6 steel exhibited a sharp drop in impact energy within the first hours of hydrogen exposure, with a 66% reduction in absorbed energy after 540 hours and reaching only 29% of the initial value by the end of the test. This behavior highlights the material's high sensitivity to hydrogen attack, reflecting its limited capacity for plastic deformation under such conditions. The predominant fracture mechanism may be associated with the nucleation and coalescence of methane bubbles and cracks, especially at grain boundaries and regions with non-metallic inclusions, which act as preferred sites for stress concentration and failure initiation.

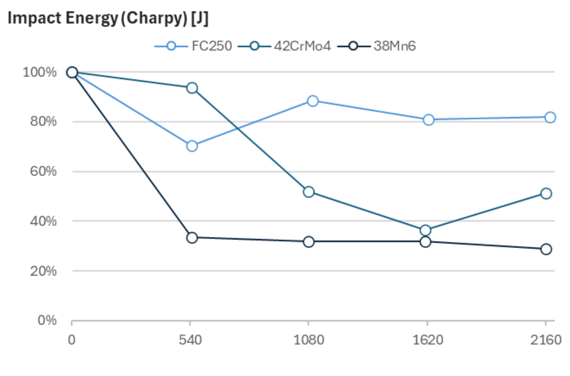

Figure 5. Percentage reduction in Charpy energy after up to 2,160 hours of hydrogen exposure

The 42CrMo4 steel also exhibited a significant reduction in impact resistance over the course of exposure. Although it reached values similar to those of the 38Mn6 steel at 1,620 hours of exposition, this point may represent an outlier, given the high variability inherent in impact testing. Nevertheless, after 2,160 hours, the material exhibited an approximate 50% reduction in toughness, highlighting the progressive damage caused by hydrogen attack and the associated formation of methane along grain boundaries.

Consistent with the tensile results, the FC250 cast iron also showed the best performance in the impact tests. Besides an initial significant drop – possibly related to an outlier – the material exhibited stable behavior, with less than a 20% reduction in its fracture toughness at the end of the exposure period. This behavior can be attributed to typical characteristics of cast irons, particularly the presence of graphite, which plays a key role in mitigating hydrogen-related degradation, and, potentially, the high silicon content. Graphite particles limit hydrogen mobility by acting as high-energy traps, a behavior reinforced by their greater thermodynamic stability compared to cementite; additionally, silicon contributes by lowering hydrogen solubility in the metal matrix. The combined action of these mechanisms favors microstructural stability and significantly contributes to the high temperature hydrogen attack resistance of cast irons.

COMMERCIAL HYDROGEN ENGINE COMBUSTION CONCEPTS

For commercial applications, various hydrogen combustion concepts have been developed and show potential for large-scale implementation. multi-point injection (MPI) represents the simplest implementation solution, providing good mixture formation and low combustion temperatures, resulting in reduced NO_x emissions. However, due to hydrogen's low minimum ignition energy and wide flammability limits, hydrogen engines with MPI technology are more susceptible to abnormal combustion phenomena, such as knocking and backfiring. These effects limit the feasible compression ratio, consequently restricting the efficiency of engines using this technology.

An alternative to mitigate the risk of knocking and backfiring in hydrogen engines is the use of low-pressure direct injection (LPDI) technology. While this configuration reduces the risk of premature ignition, LPDI engines also operate under the Otto cycle, which may limit thermal efficiency.

The high auto-ignition temperature of hydrogen enables its use in engines with high compression ratios. This characteristic is exploited in high-pressure direct injection (HPDI) systems, allowing the development of hydrogen engines with high efficiency and compression ratios typical of Diesel cycle engines [10,15,25–26]. However, considering the pressures typically used in heavy-duty vehicles, the auto-ignition temperature of hydrogen is too high for combustion to be controlled by simply increasing compression. Moreover, hydrogen's wide flammability limit and low ignition energy make controlling combustion under high-pressure conditions challenging. To overcome these barriers, additional measures can be employed in HPDI engines, such as the use of glow plugs or pilot fluids that act as ignition promoters.

When comparing the results of the present study with the mechanical and operational requirements internationally established for hydrogen internal combustion engines, it is observed that the currently available cast iron alloys are capable of satisfactorily meeting the demands of early-stage technologies, especially in MPI and LPDI configurations, where typical peak cylinder pressure (PCP) values range from 170 to 180 bar. Under these conditions, characterized by moderate pressures and temperatures, the stable performance of cast irons against hydrogen-induced damage indicates their technical viability as a long-term structural solution.

However, the technological trend in hydrogen combustion points towards higher mechanical and thermal loads, e.g. the incorporation of high-pressure direct injection (HPDI) systems, where PCP can reach levels between 270 and 280 bar. These operational conditions impose significantly more stringent demands on structural materials, requiring greater mechanical strength and stability against hydrogen's effects. In this context, the use of high-performance cast irons, such as compacted graphite iron (CGI), emerges as a promising strategy. CGI exhibits an optimized microstructure, providing a better combination of mechanical strength and toughness, enabling it to withstand high thermomechanical stresses. Furthermore, the presence of graphite, highly stable cementite, and a potentially beneficial high silicon content significantly reduce the material's susceptibility to hydrogen damage by acting as barriers to hydrogen diffusion and permeation into the metallic matrix. However, in certain CGI grades, the presence and distribution of hardened phases may locally increase vulnerability to hydrogen-related degradation, underscoring the importance of further alloy development to enhance both mechanical performance and hydrogen resistance.

To address these challenges, the development of specific CGI alloys is recommended, incorporating thermodynamically stable carbides, carefully controlled silicon levels, and optimized graphite morphology to maximize hydrogen trapping and improve overall resistance to hydrogen attack.

CONCLUSION

The results of this study demonstrate that cast irons, particularly FC250, outperform the forged steels 38Mn6 and 42CrMo4 in hydrogen-rich environments, excelling in tensile strength and fracture toughness. Even without specific optimizations for hydrogen attack resistance, FC250 maintained stable mechanical properties after 2,160 hours of exposure, with a reduction of less than 20% in impact energy and only 15% in tensile strength. This behavior is primarily attributed to the presence of graphite in the microstructure, which acts as high-energy traps for hydrogen and significantly reduces its diffusion within the metallic matrix.

In contrast, the forged steels exhibited significant degradation, showing greater susceptibility to embrittlement, even in the case of 42CrMo4, which contains alloying elements traditionally associated with mitigating this effect. These findings indicate that cast iron alloys can offer a promising alternative in critical hydrogen applications, combining low cost, processability, and adequate mechanical strength for high-durability hydrogen combustion engines.

In the context of the growing adoption of hydrogen engines, the results of this study provide valuable insights for material selection, potentially paving the way for the use of cast irons in components typically made from forged steels, such as crankshafts, camshafts, pistons, connecting rods, and gears.

For hydrogen engine blocks and heads, cast irons remain the most suitable materials due to their ideal combination of mechanical strength, durability, cost-effectiveness, and hydrogen damage resistance. Gray cast iron alloys should be able to meet the demands of hydrogen engines, particularly in systems using multi-point injection (MPI) and low-pressure direct injection (LPDI) technologies. In the context of high-pressure direct injection (HPDI) technologies, the research identifies compacted graphite iron (CGI) as a promising alternative, due to its mechanical robustness and the possibility of developing specifically engineered alloys with enhanced resistance to hydrogen-induced damage – features that make it particularly suitable for the extreme thermomechanical demands of these systems.

REFERENCES

[1] IPCC (1992). The IPCC 1990 and 1992 Assessments. World Meteorological Organization and United Nations Environment Programme.

[2] UN (2015). Paris Agreement. *United Nations*.

[3] UNCTAD (2024). Countries agree $300 billion by 2035 for new climate finance goal – what next? *UN Trade & Development.*

[4] Crippa, M., et al. (2024). GHG emissions of all world countries. *JRC Science for Policy Report*. Publications Office of the European Union, Luxembourg.

[5] Restrepo-Flórez, J. M., Cuello-Penaloza, P., Canales, E., Witkowski, D., Rothamer, D. A., Huber, G. W., & Maravelias, C. T. (2023). Ethanol to diesel: a sustainable

alternative for the heavy-duty transportation sector. *Sustainable Energy & Fuels*, *7(3)*, 693-707.

[6] Noussan, M. (2023). The use of biomethane in internal combustion engines for public transport decarbonization: a case study. *Energies*, *16(24)*, 7995.

[7] Chakraborty, S. et al. (2022). Hydrogen energy as future of sustainable mobility. *Frontiers in Energy Research*, *10*, 893475.

[8] Dash, S. K., et al. (2022). Hydrogen fuel for future mobility: Challenges and future aspects. *Sustainability*, *14(14)*, 8285.

[9] Jones, A., & Neilson, M. (2021). Battery electric vs hydrogen – Which is the future for electric vehicles. *Murgitroyd*.

[10] Tupy (2021). TUPY, Westport Fuel Systems and AVL work in partnership to develop world's most efficient hydrogen internal combustion engine pilot.

[11] MAN (2022). MAN Engines: The first dual fuel hydrogen engines in use on a work boat. MAN Newsroom Corporate.

[12] Cummins (2022). Cummins Inc. Debuts 15-Liter Hydrogen Engine at ACT Expo.

[13] DAF (2021). DAF'S XF Hydrogen wins 2022 truck innovation award. International Truck of the Year.

[14] Mercedes (2023). Hydrogen-powered Unimog as a climate-neutral commercial vehicle when in operation.

[15] Scania (2021). Scania and Westport Fuel Systems will cooperate in hydrogen research project.

[16] Iveco (2023). O novo motor de combustão de hidrogênio XC13 da FPT Industrials faz sua estreia em campo na copa do mundo de esqui de Flachau junto com a PRINOTH.

[17] Volvo Penta (2022). Volvo Penta and CMB. TECH partner on dual-fuel hydrogen engines.

[18] Ford Otosan (2024). Ford Trucks Achieves First Ignition of Multi-Cylinder Hydrogen Engine.

[19] MTU (2023). Hydrogen – Making combustion engines green.

[20] Rolls-Royce (2022). Rolls-Royce and easyJet set new world first.

[21] Hyundai (2025). HD Hyundai Infracore Hydrogen Engine Proven Performance in Frigid Temperatures of -20 degrees Celsius.

[22] Mitsubishi Heavy Industries (2025). MHIET Achieves Rated Operation of a 6-Cylinder 500kW-class Hydrogen Engine Generator Set – Demonstration Tests at Company's Sagamihara Plant.

[23] Deutz (2021). DEUTZ TCG 7.8 Hydrogen – Hydrogen-combustion engine.

[24] Deutz (2024). DEUTZ joins consortium to develop hydrogen engines for off-highway applications.

[25] AVL (2021). TUPY, Westport Fuel Systems and AVL to Collaborate in Demonstration of World's Most Efficient Hydrogen-Fueled Internal Combustion Engine.

[26] WSF (2022). Westport and Scania Announce Impressive Test Results of H_2 HPDI™ Fuel System for Heavy-Duty Transport.

[27] JCB (2024). Previewing the JCB hydrogen generator.

[28] Kawasaki (2024). World's First Public Demonstration Run of a Hydrogen Engine Motorcycle by a Mass-Production Motorcycle Manufacturer.

[29] Miller, B. A., Shipley, R. J., Parrington, R. J., and Dennies, D. P. (2002). ASM Materials Handbook, Metals Handbook, 10th Edition, Volume 11, *Failure Analysis and Prevention*, ASM International, Ohio.

[30] Carter, T. J., and Cornish, L. A. Hydrogen in Metals, *Engineering Failure Analysis*, Vol. 8, No. 2, 2001, pp. 113-121.

[31] Louthan, M. R. (2008). Hydrogen embrittlement of metals: a primer for the failure analyst. *Journal of Failure Analysis and Prevention*, *8*, 289-307.

[32] Whiteman, M. B., & Troiano, A. R. (1965). Hydrogen embrittlement of austenitic stainless steel. *Corrosion*, *21(2)*, 53-56.

[33] Nouri, A., & Wen, C. (2021). Stainless steels in orthopedics. *Structural biomaterials* (pp. 67-101). Woodhead Publishing.

[34] Fashu, S., & Trabadelo, V. (2023). A critical review on development, performance and selection of stainless steels and nickel alloys for the wet phosphoric acid process. *Materials & Design*, *227*, 111739.

[35] Hsu, K. L., Ahn, T. M., & Rigney, D. A. (1980). Friction, wear and microstructure of unlubricated austenitic stainless steels. *Wear*, *60(1)*, 13-37.

[36] Gallego, J. D., Malo, I., López, I., Gonzalez, C. D., & de Yebes, O. (2015). Thermal Conductivity and Electrical Loss of Thin Wall millimeter wave stainless steel waveguides. IT-CDT 2015-14, Observatorio de Yebes Guadalajara.

[37] Ban, H., & Shi, G. (2018). A review of research on high-strength steel structures. *Proceedings of the Institution of Civil Engineers-Structures and Buildings*, *171(8)*, 625-641.

[38] Pradhan, A., Vishwakarma, M., & Dwivedi, S. K. (2020). A review: The impact of hydrogen embrittlement on the fatigue strength of high strength steel. *Materials Today: Proceedings*, *26*, 3015-3019.

[39] Guesser, W. L. (2009). Propriedades mecânicas dos ferros fundidos. *Editora Blucher*.

[40] Angus, H. T. (2013). Cast iron: physical and engineering properties. *Elsevier*.

[41] Wu, R., Ahlström, J., Magnusson, H., Frisk, K., Martinsson, A., & Kimab, S. (2015). Charging, degassing

and distribution of hydrogen in cast iron. Stockholm: Svensk kärnbränslehantering (SKB).

[42] Lee, S. M., Park, I. J., Jung, J. G., & Lee, Y. K. (2016). The effect of Si on hydrogen embrittlement of Fe-18Mn-0.6 C-xSi twinning-induced plasticity steels. *Acta Materialia, 103*, 264-272.

[43] Ke, N., Huang, H., Wang, F., Dong, B., Huang, A., Hao, L., & Xu, X. (2023). Study on the hydrogen barrier performance of the SiOC coating. *International Journal of Hydrogen Energy, 48(22)*, 8286-8295.

[44] Petrova, E. F., Rogov, A. I., Kozlenkov, E. M., & Shvartsman, L. A. (1988). Effect of silicon on the resistance of steel to hydrogen cracking. *Prot. Met. (Engl. Transl.); 23(6).*

[45] Elboujdaini, M., & Hay, M. G. (2018). Review of the effect of hydrogen on mechanical properties of low strength steels in oil and gas applications. Strength, *Fracture and Complexity, 11(2-3)*, 169-184.

[46] Azevedo, C. R. (2007). Failure analysis of a crude oil pipeline. *Engineering Failure Analysis, 14(6),* 978-994.

[47] Sahiluoma, P., Yagodzinskyy, Y., Forsström, A., Hänninen, H., & Bossuyt, S. (2021). Hydrogen embrittlement of nodular cast iron. *Materials and Corrosion, 72(1-2)*, 245-254.

[48] Goyal, H., Jones, P., Bajwa, A., Parsons, D., Akehurst, S., Davy, M. H., ... & Esposito, S. (2024). Design trends and challenges in hydrogen direct injection (H2DI) internal combustion engines – A review. *International Journal of Hydrogen Energy, 86,* 1179-1194.

[49] Pressouyre, G. M. (1980). Trap theory of hydrogen embrittlement. *Acta Metallurgica, 28(7),* 895-911.

[50] Hagi, H., Hayashi, Y., & Ohtani, N. (1979). Diffusion coefficient of hydrogen in pure iron between 230 and 300 K. *Transactions of the Japan Institute of Metals, 20(7),* 349-357.

[51] Choo, W. Y., & Lee, J. Y. (1982). Thermal analysis of trapped hydrogen in pure iron. *Metallurgical Transactions A, 13,* 135-140.

[52] Oger, L., Malard, B., Odemer, G., Peguet, L., & Blanc, C. (2019). Influence of dislocations on hydrogen diffusion and trapping in an Al-Zn-Mg aluminium alloy. *Materials & Design, 180*, 107901.

[53] Cho, S., Kim, G. I., Ko, S. J., Yoo, J. S., Jung, Y. S., Yoo, Y. H., & Kim, J. G. (2022). Comparison of hydrogen embrittlement susceptibility of different types of advanced high-strength steels. *Materials, 15(9),* 3406.

[54] Roth, J., Scherzer, B. M. U., Blewer, R. S., Brice, D. K., Picraux, S. T., & Wampler, W. R. (1980). Trapping, detrapping and replacement of keV hydrogen implanted into graphite. *Journal of Nuclear Materials, 93,* 601-607.

[55] Kanashenko, S. L., Gorodetsky, A. E., Chernikov, V. N., Markin, A. V., Zakharov, A. P., Doyle, B. L., & Wampler, W. R. (1996). Hydrogen adsorption on and solubility in graphites. *Journal of nuclear materials, 233,* 1207-1212.

[56] Turola, J., Obara, R. B., Ferrarese, A., Albaneze, A. F., & de Souza Cabezas, C. (2024). Microstructure of cast iron resistant to hydrogen embrittlement (No. 2023-36-0063). *SAE Technical Paper.*

[57] Takai, K. I., Chiba, Y., Noguchi, K., & Nozue, A. (2002). Visualization of the hydrogen desorption process from ferrite, pearlite, and graphite by secondary ion mass spectrometry. *Metallurgical and Materials Transactions A, 33,* 2659-2665.

[58] Yoshimoto, T., Matsuo, T., & Ikeda, T. (2019). The effect of graphite size on hydrogen absorption and tensile properties of ferritic ductile cast iron. *Procedia Structural Integrity, 14,* 18-25.

[59] Chicet, D. L., & Cojocaru-Filipiuc, V. (2014). Silicon influence on the cast iron structure. *Applied Mechanics and Materials, 659,* 46-50.

[60] ISO 6892-1 (2009). Metallic Materials – Tensile testing – Part 1: Method of test at room temperature 2009:70

[61] ASTM E23 (2024). Standard Test Methods for Notched Bar Impact Testing of Metallic Materials.

[62] Lee, J., Lee, T., Mun, D. J., Bae, C. M., & Lee, C. S. (2019). Comparative study on the effects of Cr, V, and Mo carbides for hydrogen-embrittlement resistance of tempered martensitic steel. *Scientific Reports, 9(1),* 5219.